applied sciences

MDPI

Article

Development of Far-UVC-Based Surface Disinfection Prototype for Public Buses

Darius Drungilas *, Mindaugas Kurmis, Arturas Tadzijevas, Zydrunas Lukosius, Deivydas Sapalas, Valdas Jankunas, Arvydas Martinkenas, Rimantas Didziokas and Jurate Gruode

Marine Research Institute, Klaipeda University, H. Manto Str. 84, LT-92294 Klaipeda, Lithuania
* Correspondence: darius.drungilas@ku.lt

Abstract: This paper presents a prototype of a disinfection system for public transport specifically aiming to disinfect surfaces contaminated with the SARS-CoV-2 virus on buses using 222 nm wavelength far-ultraviolet light (far-UVC). Our study involved testing the developed technical system installed in a 12 m long M3 category urban bus, an investigation of optimal far-UVC light angles, and the determination of disinfection parameters for bus seat disinfection. The study identified the ideal positioning of a light source for effective disinfection and analyzed three disinfection scenarios, considering zone coverage, disinfection time, and energy demand. A subsystem employing real-time occupancy monitoring enhances the disinfection process in crowded areas of buses. An energy efficiency assessment model is proposed for optimizing energy consumption. Furthermore, the energy consumption analyses in different disinfection scenarios provide valuable insights for optimizing energy usage in public transport disinfection.

Keywords: far-UVC; surface disinfection; SARS-CoV-2; public transport

check for updates

Citation: Drungilas, D.; Kurmis, M.; Tadzijevas, A.; Lukosius, Z.; Sapalas, D.; Jankunas, V.; Martinkenas, A.; Didziokas, R.; Gruode, J. Development of Far-UVC-Based Surface Disinfection Prototype for Public Buses. *Appl. Sci.* **2023**, *13*, 8501. https://doi.org/10.3390/app13148501

Academic Editor: Enoch Y. Park

Received: 29 June 2023
Revised: 18 July 2023
Accepted: 20 July 2023
Published: 23 July 2023

1. Introduction

The outbreak of the COVID-19 pandemic has brought public health and safety to the forefront of global concerns. The rapid transmission of the SARS-CoV-2 virus, which causes COVID-19, has underscored the importance of implementing effective measures to prevent and control the spread of infectious diseases. Among the various settings that require attention, public transport systems have emerged as potential hotspots for viral transmission due to the close proximity of passengers and frequent contact with shared surfaces.

In recent years, there has been a growing body of research exploring various aspects of the surface and airborne transmission of viral pathogens including SARS-CoV-2 in public transport. Moreno et al. conducted a study tracing surface and airborne SARS-CoV-2 RNA inside public buses and subway trains [1]. The study collected 99 samples from inside Barcelona buses and subway trains. The results showed that the presence of viral RNA fragments in buses was higher than in trains, and relatively higher concentrations of viral RNA fragments were found on support bars than in ambient air inside the vehicles. Public transportation systems can reduce the transmission of SARS-CoV-2 by implementing specific mitigation solutions such as the appropriate filtration of recirculated air and simultaneous use of FFP2 masks, especially in long-distance buses [2]. For urban buses, the maximum occupancy needs to be reduced to maintain a reproductive number of less than 1. However, it is very difficult to achieve such measures in highly populated areas.

In response to this unprecedented challenge, innovative technologies have been developed to enhance disinfection protocols within public transport environments. Ultraviolet (UV) light-based systems, known for their ability to rapidly eliminate harmful microorganisms, have gained significant attention as promising solutions. Specifically, the use of UVC light at a wavelength of 222 nanometers (nm) has demonstrated efficient pathogen inactivation while minimizing risks to human health [3–7]. According to a review on UVC disinfection [8], UVC-based technologies offer several advantages compared to traditional chemical-based disinfection approaches. They are environmentally friendly, have high levels of pathogen reduction (higher than 99.9%), and reduce the manual cleaning and equipment maintenance provided by manpower, which make them very suitable for the disinfection of public transport systems.

Another study [9] proved the effectiveness of UV light in inactivating SARS-CoV-2, the virus responsible for COVID-19, in human saliva. The study compared the efficacy of a commercial filtered krypton chlorine (KrCl) excimer light source emitting a peak wavelength of 222 nm to that of a conventional germicidal lamp emitting UV 254 nm. The results showed that both UV wavelengths could effectively reduce the viral load, but the UV 254 nm had a greater capacity to inactivate the virus.

The systematic review by Ramos et al. [10] assessed the effectiveness and safety of UVC sterilization in reducing nosocomial infections in hospitals. After analyzing 17 eligible studies from 2010 to 2020, positive results were observed when UVC irradiation was used alongside existing cleaning protocols. UVC demonstrated potent germicidal effects against viruses, Methicillin-resistant *Staphylococcus aureus* (MRSA), and Vancomycin-resistant *Enterococci* (VRE).

UVC Disinfection Robots have gained prominence for their ability to employ UVC light, which possesses germicidal properties, to disinfect surfaces and air, offering automated and precise disinfection capabilities in various settings including hospitals, public spaces, and transportation systems [11–13]. By emitting a specific wavelength of UVC light, these robots can penetrate the DNA of viruses and bacteria, rendering them inactive and incapable of reproduction. This technology has proven particularly effective in hospitals, laboratories, and public spaces, where comprehensive disinfection is vital.

Numerous studies have been conducted to investigate the efficacy and practicality of UVC disinfection robots in diverse settings, especially hospitals. A summary of these studies is provided in Table 1.

Table 1. Summary of robotic UVC disinfection research.

Scheme	UV Wavelength	Objective	Findings
Tru-D™ room disinfection device [14].	Not specified	Assess the efficacy of a Tru-D UVC room decontamination device	The successful eradication of organisms in an unoccupied operating theatre was accomplished.
UV-C Disinfection Robot Field Study [15]	254 nm	Evaluate the effectiveness and usability of a UVC disinfection robot in hospital setting	The robot was not found suitable for integration into hospital's cleaning procedures; it had an insufficient UVC irradiation cycle for pathogens with enhanced environmental resilience; it was effective in reducing the microbial burden on hospital surfaces.
Whole-Room UVGI Device [16]	254 nm	Investigate the effectiveness of whole-room UVGI devices in controlling surface-borne pathogens	*Bacillus atrophaeus* spores serve as suitable model organisms for testing the influence of shadows on the inactivation efficacy of mobile whole-room UVGI devices.
COVID-19 Disinfection Robot [17]	254 nm	Develop a robot specifically designed for disinfecting COVID-19 in complex indoor settings	The robot incorporates UVC lamps, features a six-degree-of-freedom arm and a wheeled platform, has a method for calculating surface dosage and creating a disinfection map, and showed successful testing results in a representative indoor environment.
UVC-PURGE Robot [18]	254 nm	Evaluate the performance of the UVC-PURGE robot in combating COVID-19	The robot effectively disinfects surfaces, destroys SARS-CoV-2 virus, and demonstrates navigational capabilities; it is highly usable and cost-effective compared to other UVC disinfection robots.

Table 1. *Cont.*

Scheme	UV Wavelength	Objective	Findings
UVC and far-UVC light disinfection ground robot [19]	222 nm and 254 nm	Investigate the feasibility and effectiveness of using autonomous mobile robots equipped with 254 nm UVC and 222 nm far-UVC light towers	The study demonstrated the feasibility and promising disinfection performance of autonomous mobile robots equipped with UV light towers using 254 nm UVC and 222 nm far-UVC lights, effectively sterilizing the coronavirus on irradiated surfaces, eliminating the need for space evacuation during the disinfection process.
Far-UVC Disinfection with Robotic Mobile Manipulator [20]	222 nm	Introduce a cost-effective germicidal system that utilizes Ultraviolet Germicidal Irradiation (UVGI) to disinfect high contact surfaces and combat infectious disease agents such as viruses, bacteria, and fungi	The G-robot, which is a human-safe mobile manipulator for UV disinfection, was presented, and it demonstrated its efficacy in terms of dosage distribution, energy consumption, and real-world application. The G-robot is able to be used in a human presence, and it shows its improved disinfection effectiveness in cluttered and shadowed spaces.
COVID-Bot Autonomous Sanitizing Robot [21]	Not specified	Introduce an autonomous sanitizing robotic platform utilizing UVC radiation	The COVID-Bot effectively disinfects surfaces using UVC radiation; it operates autonomously and covers significant surface area in approximately 8 min.
UVC-Based Disinfection Robot [22]	Not specified	Develop a UVC-based disinfection robot with mobile platform and six-axis robotic arm	The robot emphasizes remote control, path planning, data monitoring, and the customization of disinfection functions.
Other Studies [23–25]	Not specified, 254 nm	Assess the performance, efficiency, and safety of UVC disinfection robots; optimize design and functionality	Efforts to enhance the mobility, navigation capabilities, and integration of advanced sensors and AI algorithms.

Despite the extensive research conducted on UVC disinfection systems, recent studies have shifted their focus towards investigating the effects of UVC radiation exposure on various materials. For example, one study examined the effects of UVC radiation exposure on materials (fabric and plastic) commonly used in aircraft cabins. The study found that cumulative damage from frequent UVC radiation application has no significant effect on flame retardancy up to 269 J/cm^2 of dose, and no effect on tensile or tear strength up to 191 J/cm^2. However, changes in color or appearance can occur at lower doses, and a limit of 40 J/cm^2 was proposed to avoid perceptible changes in appearance [26]. Another investigation on UVC's effect on materials was conducted in our previous research [27], where we found that the use of far-UVC radiation with a specific wavelength of 222 nm for disinfection can have significant negative effects on the mechanical and visual properties of the surfaces to be disinfected. The results of the study showed that far-UVC radiation at 222 nm causes significant color degradation in all the polymeric materials tested. The degree of color degradation varies depending on the type of polymeric material and the duration of exposure to far-UVC radiation.

As ongoing research and development continues to refine UVC disinfection robot systems, these technologies are expected to play an increasingly important role in public health and infection control strategies. The collective findings from these studies will guide the deployment and optimization of UVC disinfection robots, leading to safer and healthier environments for people worldwide.

The aim of this scientific article is to present a comprehensive evaluation of the reliability and functionality of a specially developed prototype of a public transport disinfection system using 222 nm far-UVC light. The investigation and evaluation focus on the critical aspect of efficient surface disinfection with minimal energy consumption. By analyzing these factors, we aim to provide insight into the system's practicality and its potential to effectively protect public health while ensuring sustainable operation in the face of ongoing infectious disease challenges.

2. Materials and Methods

2.1. Design of Far-UVC-based Disinfection System Prototype for Public Transport

The main objective of the far-UVC disinfection system is to reduce severe acute respiratory syndrome coronavirus 2 (SARS-CoV-2) surface contamination in public buses. A prototype of the disinfection system was developed based on previous studies [6,7] demonstrating the disinfection effect of far-UVC irradiation. However, high doses of UV radiation also have a negative effect on the mechanical and aesthetic properties of the surfaces being disinfected [27]. Based on these assumptions, the disinfection system must operate in an optimal mode to inactivate viruses with the least negative impact on surfaces. This can be achieved by monitoring the occupancy of each area in a bus during a journey and selecting the optimum dose of far-UVC radiation in each area. Figure 1 shows the main components of a prototype of a disinfection system comprising a computer vision system and far-UVC radiation control system.

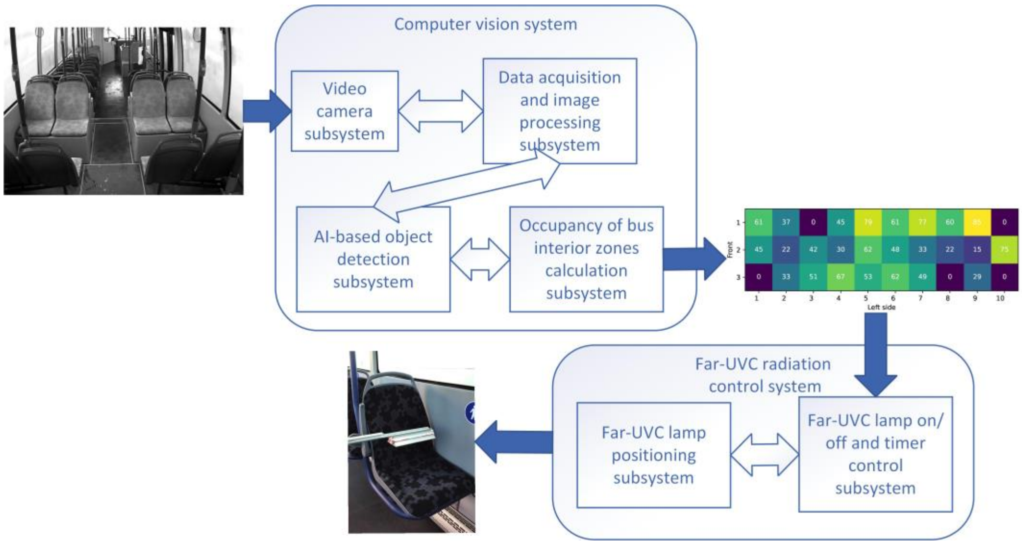

Figure 1. Block diagram of a prototypical far-UVC disinfection system.

The computer vision system uses a video camera to capture the image of the bus interior, which is processed using filters and noise reduction algorithms. An object detection algorithm is then used to detect passengers and calculate the occupancy of the bus interior. Disinfection of the bus interior is performed by a far-UVC radiation control system, which controls the exposure time and positions the lamps according to the occupancy of the bus interior zones.

The computer vision system starts the process by capturing an image of the bus interior. It then defines a region of interest that includes the bus seats. The image is then processed by resizing, noise removal, sharpening, histogram equalization, and normalization. In the next step, the image is fed to a trained YOLO v7 model [28], which is capable of distinguishing only people in a video frame. Based on the detected persons, a list of all passenger coordinates in the video frame is generated, and the occupancy of the bus interior zones is calculated by outputting a heat map related to the bus interior zone coordinates.

Figure 2 shows a detailed flowchart of the computer vision system.

The far-UVC light sources of the prototype developed consisted of two Quantadose B-Series DF28B-B3 (Guangdong Excimer Optoelectronics Technology, Jiangmen, China) 20-watt filtered 222 nm far-UVC excimer lamp modules fitted with 222 nm bandpass filters and enclosed in protective housings to ensure lamp integrity and cooling. These lamp modules were powered by a dedicated 40W high-voltage excimer lamp electronic power supply. To increase the precision and accuracy of the far-UVC exposure, bandpass filters were used within the lamp modules to ensure that only the desired wavelength of UV light was emitted. In addition, the prototype incorporated a mechanism controlled by a microcontroller and driven by stepper motors to manipulate the distance, position, and movement of each lamp module. By adjusting the distance between the irradiated surface and the far-UVC light source, the intensity of the far-UVC light exposure could be varied. The spectral characteristics of the far-UVC lamps were evaluated using an Avantes AvaSpec ULS2048 CL spectroscope (manufacturer AVANTES B.V., Apeldoorn, the Netherlands). The spectrogram of the direct light emitted by the lamps, which clearly shows a dominant wavelength of 222 nm, is shown in Figure 3.

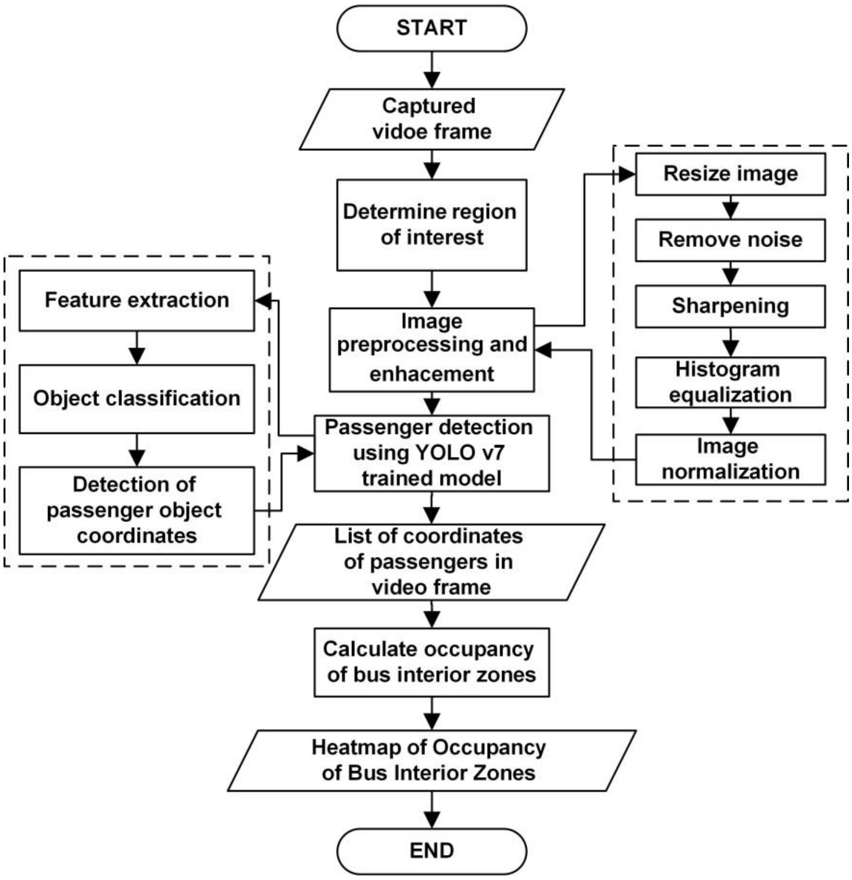

Figure 2. Flowchart of computer vision system for bus interior occupancy detection.

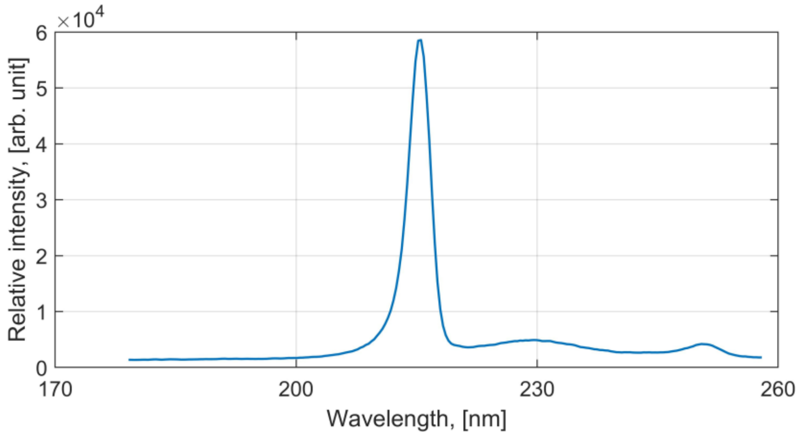

Figure 3. Spectrogram of far-UVC lamp modules used in developed prototype of disinfection system.

A X1-5 optometer (manufacturer Gigahertz Optik GmbH, Tuerkenfeld in Munich, Germany) equipped with a calibrated 222 nm sensor was used to measure radiant exposure. The far-UVC lamps were mounted on a robotic structure that allowed the lamps to be positioned in the appropriate row of bus seats and lowered to the seat surface to achieve the required amount of irradiation on the surface to be disinfected (Figure 4). To disinfect one row, the system developed had 2 disinfection lamps.

Figure 4. Far-UVC disinfection system installed in M3 category city bus: 1. Robotic lamp positioning and lifting/lowering system; 2. Rotating lamp holder; 3. Far-UVC lamps.

2.2. Public Transport Disinfection Scenarios

A 12 m long M3 city bus typically has 10 rows of seats, which were used as disinfection zones in this study. By evaluating the occupancy of the interior of the bus, it is possible to disinfect the bus during the journey by disinfecting rows of seats that have become vacant or to disinfect at the end of the journey when the bus is completely empty of passengers. The most frequently touched areas of the bus seats are shown in Figure 5 and during the disinfection process. According to previous studies [6,7], it is important that these areas receive at least 2 mJ/cm^2 of irradiation to inactivate the SARS-CoV-2 virus.

Figure 5. Measurement points for the far-UVC irradiation of bus seats.

For the fastest disinfection and lowest energy consumption, three disinfection scenarios can be analyzed for each row of seats.

2.2.1. Scenario 1

Experiments were carried out to determine both the distance at which the far-UVC light source of the disinfection system should be positioned as well as the intensity and direction of the radiation. It was found that an even, optimum distribution of irradiation is achieved when the light source is directed vertically downwards, the center of the light source coincides with the center of the seat, and the source is vertically 75 cm from the seat and 25 cm from the center of the backrest (Figure 6).

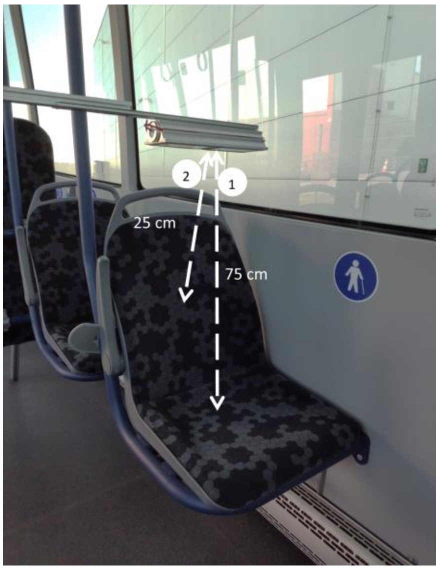

Figure 6. Far-UVC lamp positioning according to scenario 1.

Considering that the backrest is tilted, the horizontal distance is measured from the center of the backrest. The disinfection system is fixed so that 2 mJ/cm^2 is achieved in the lowest irradiance zones.

2.2.2. Scenario 2

At measurement points 1, 2, and 3, the far-UVC lamps should be positioned at three different heights until the required irradiance (2 mJ/cm^2) is achieved (Figure 5). The lamps are positioned at 100, 50, and 25 cm from the bottom of the seat (see Figure 7). ‘

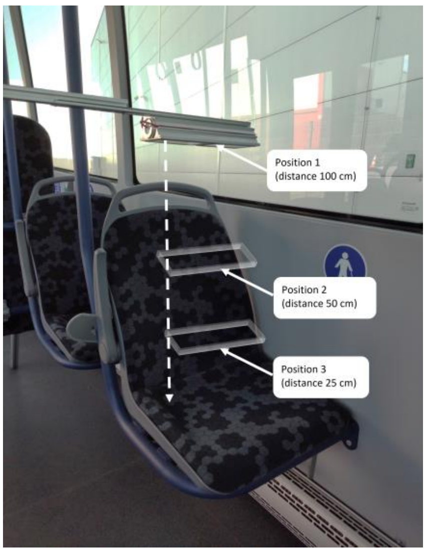

Figure 7. Far-UVC lamp positioning according to scenario 2.

2.2.3. Scenario 3

The far-UVC lamps were lowered at a constant speed (2.5 cm/min) until the irradiance of 2 mJ/cm^2 was reached at measurement points 1, 2, and 3 (Figure 5). The initial position of the lamps (90 cm from the bottom of the seat) was determined experimentally after evaluating the angle of illumination and the distribution of the irradiation (Figure 8).

Figure 8. Far-UVC lamp positioning according to scenario 3.

2.3. Energy Efficiency Evaluation Model

In order to select the optimal far-UVC irradiation, it is necessary to create a model that, based on the parameters of the far-UVC source and the duration of exposure, would allow simulating the energy requirements for the disinfection process. An energy efficiency assessment model is developed with the following assumptions:

1. The parameters of the electrical power supply network supplying the module remain constant over time.
2. The module has two states: connected to the electrical power supply or disconnected from it.
3. The module is passively cooled.
4. The temperature of the UVC lamp is equal to the temperature of the glass bulb of the lamp.
5. The temperature of the power supply of the module does not affect the light output of the UVC lamp.
6. The temperature of the converter of the module does not affect the light output of the UVC lamp.

The temperature in Kelvin (K) of the UVC lamp in the module is modelled by the following Equation (1):

$$T = T_S + \Delta T\left(1 - e^{k_T(t-t_S)}\right), \tag{1}$$

where t is a time (s) since the start of the simulation, t_S is the point in time (s) at which the state of the module changed, T_S is the temperature (K) of the UVC lamp at the moment when the state of the module changed, k_T is a coefficient, and ΔT is the temperature difference (K) at the moment when the state of the module changed.

The temperature difference ΔT depends on the change in module state and can be expressed as follows:

$$\Delta T = \begin{cases} T_{max} - T_S, & when\ state\ changes\ from\ OFF\ to\ ON \\ T_{amb} - T_S, & when\ state\ changes\ from\ ON\ to\ OFF' \end{cases} \tag{2}$$

where T_{amb} is the temperature of the UVC lamp before the start of the simulation, when its temperature is equal to the ambient temperature; T_{max} is the maximum temperature that the UVC lamp can reach if when the module is operated for a sufficiently long time. At the start of the simulation, the values of the model parameters are set as follows: $T_S = T_{amb}$, ΔT is calculated using Equation (2) assuming that the module changes state, and $t_S = t$.

The radiance (W/m^2) of a UVC lamp is modelled by the following equation:

$$E_e = \begin{cases} C_E + e^{k_{Ea} + \frac{k_{Eb}}{T} + k_{Ec}\log(T)}, & \textit{when state is ON} \\ 0, & \textit{when state is OFF} \end{cases}, \tag{3}$$

where C_E is a constant and k_{Ea}, k_{Eb} and k_{Ec} are coefficients.

The instantaneous electric power (W) of the module is modelled by the following Equation:

$$P = \begin{cases} C_P + k_{Pa} e^{\frac{k_{Pb}}{T + k_{Pc}}}, & \textit{when state is ON} \\ 0, & \textit{when state is OFF} \end{cases}, \tag{4}$$

where C_P is a constant and k_{Pa}, k_{Pb} and k_{Pc} are coefficients.

From the start of the simulation t_0 to the time point t_m, the power consumed (Ws) by the module is calculated thus:

$$E = \int_{t_0}^{t_m} P(t)dt, \tag{5}$$

3. Results

To ensure sufficient surface irradiation for disinfection, an evaluation of the distribution of far-UVC light irradiation on the studied surface was first carried out. For this purpose, the area of the tested irradiated surface of 400 × 600 mm was divided into 32 sectors (4 × 8), and in each sector, the irradiance was measured at different distances between the light source and the surface (20 cm, 30 cm, 40 cm, 50 cm, and 60 cm). The resulting heat maps are shown in Figure 9.

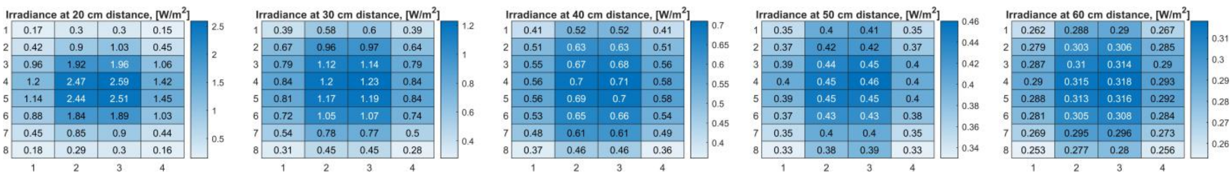

Figure 9. Heatmaps of far-UVC lamp irradiance measurements at various distances between the light source and the surface.

As we can see, at a small distance (20 cm) between the surface and the lamp, the irradiance on the surface is very unevenly distributed, with very high irradiance in the center and very low irradiance at the edges. These differences decrease as the distance increases, but the average irradiance also decreases. The dependence of the unevenness of the surface irradiance on the distance is also clearly visible after calculating the standard deviations of the sector irradiance in Figure 10.

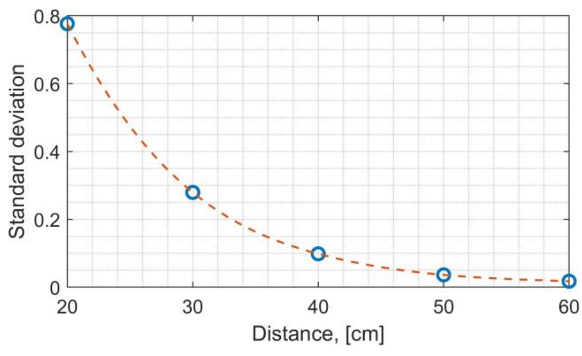

Figure 10. The standard deviations of surface sector irradiance according to distance.

The dependence of the irradiance (measured around the center of the far-UVC lamp) on the distance of the far-UVC source and the measured angle is shown in the polar diagram in Figure 11.

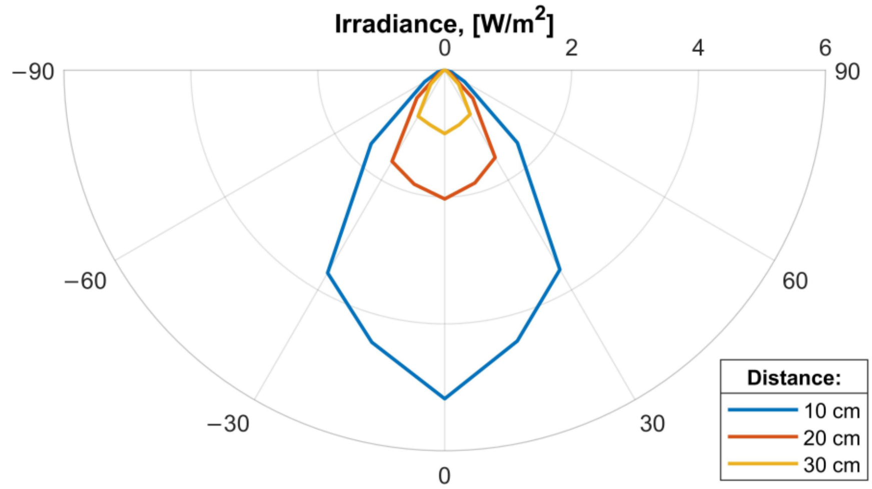

Figure 11. The irradiance at the distance of the far-UVC source and the measured angle.

We can see that the beam angle of the far-UVC lamps used in the prototype is approximately 60° and can also see how the irradiance decreases with distance. Correspondingly, the dependences of the irradiance on time and the different distances between the lamp and the surface are shown in Figures 12 and 13.

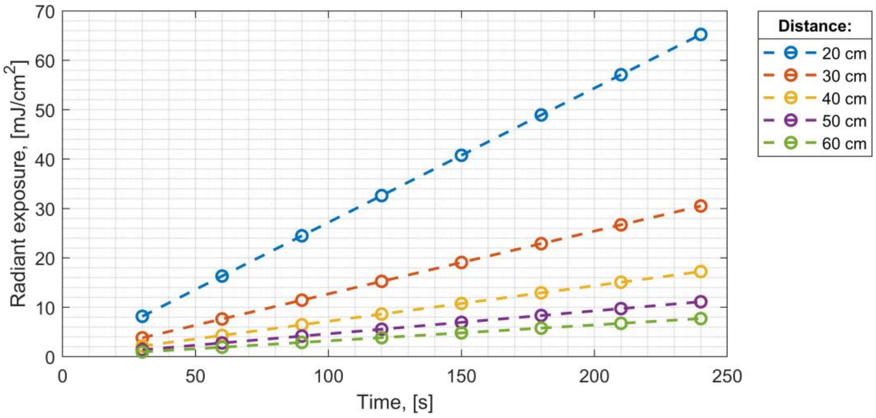

Figure 12. The dependences of radiant exposure on time and the different distances between the lamp and the surface.

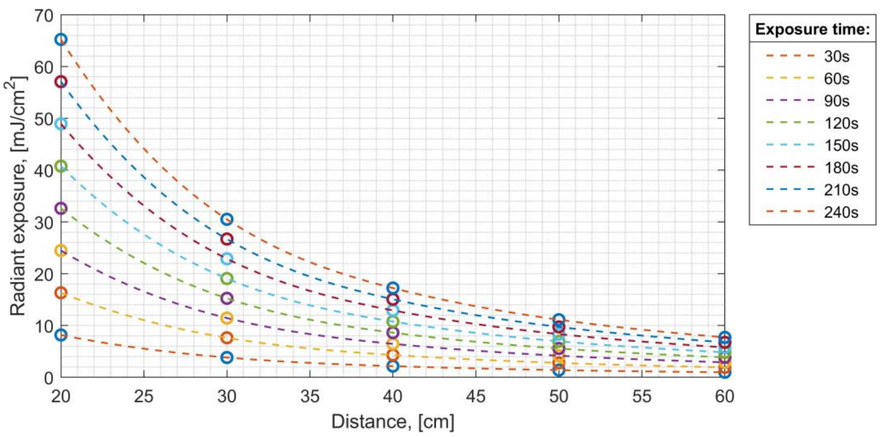

Figure 13. The dependences of radiant exposure on various distances and exposure times.

When evaluating the disinfection scenarios described above, the speed of disinfection and the amount of energy used were analyzed. The duration of disinfection for each scenario was determined to achieve 2 mJ/cm^2 radiant exposure at the measurement points. For each scenario, this was done by measuring the radiant exposure using a Gigahertz Optik, X1-5 (Gigahertz Optik GmbH, Tuerkenfeld, Germany) optometer at measurement points 1, 2, and 3.

For the disinfection of a bus row with four seats, two cases are considered for each scenario, in which two and four far-UVC lamps are used. When two lamps are used, the disinfection of the row takes more than twice as long, as each lamp has to be moved to the position of the adjacent seat, which takes 30 s. Furthermore, considering the case where the bus has ten rows and experimentally it was found that the transition of the lamp from one row to another takes 54 s, the disinfection times of all the rows of the bus can be calculated. The results are shown in Table 2. For scenarios 1 and 2, the disinfection time for a zone is determined by the longest time at the measured points. Therefore, for scenario 1, the disinfection time of 75 s is determined by measuring point 1 and for scenario 3, the disinfection time of 73 s is determined by measuring point 3. For scenario 2, the disinfection times for each position are summed.

Table 2. Scenario evaluation results.

	Scenario 1	**Scenario 2**	**Scenario 3**
Time to reach 2 mJ/cm^2 at measurement point 1	75 s	56 s	64 s
Time to reach 2 mJ/cm^2 at measurement point 2	32 s	51 s	35 s
Time to reach 2 mJ/cm^2 at measurement point 3	56 s	38 s	72 s
Row disinfection time using 4 lamps per row	75 s	190 s	72 s
Row disinfection time using 2 lamps per row	180 s	410 s	174 s
Bus disinfection time using 4 lamps per row	1236 s	2366 s	1479 s
Bus disinfection time using 2 lamps per row	2286 s	4142 s	2232 s
Total energy consumption using 4 lamps per row	109.8 Wh	195.9 Wh	112.3 Wh
Total energy consumption using 2 lamps per row	111.3 Wh	197.4 Wh	116.1 Wh

The electrical power requirements for the disinfection system are modelled based on the Energy Efficiency Assessment model. The modelling also considers that 2 NEMA34 and 2 NEMA23 stepper motors are used to move the lamps to the next row and to the adjacent seat, and to raise and lower the lamps. The results are shown in Figures 14–16.

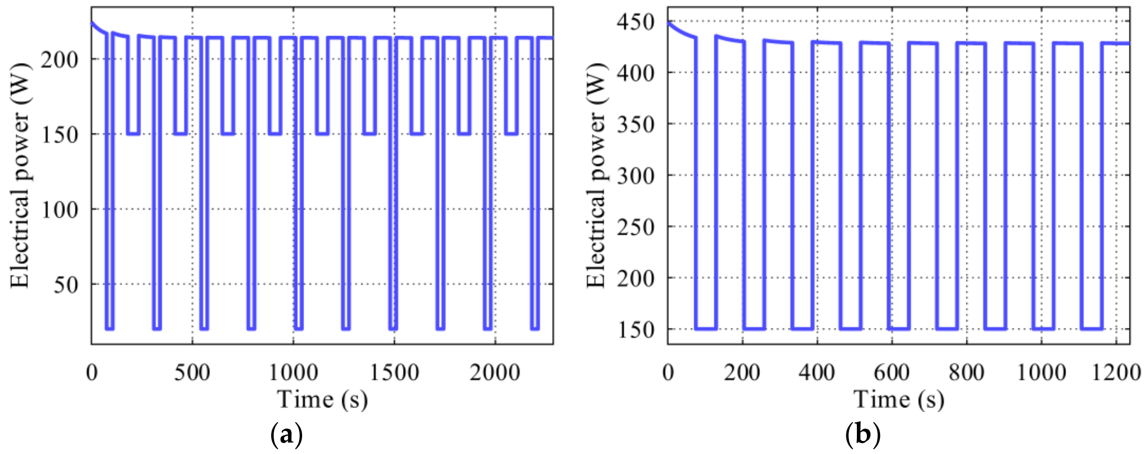

Figure 14. Electrical power consumption according to disinfection scenario 1 using two far-UVC lamps (**a**) and four far-UVC lamps (**b**).

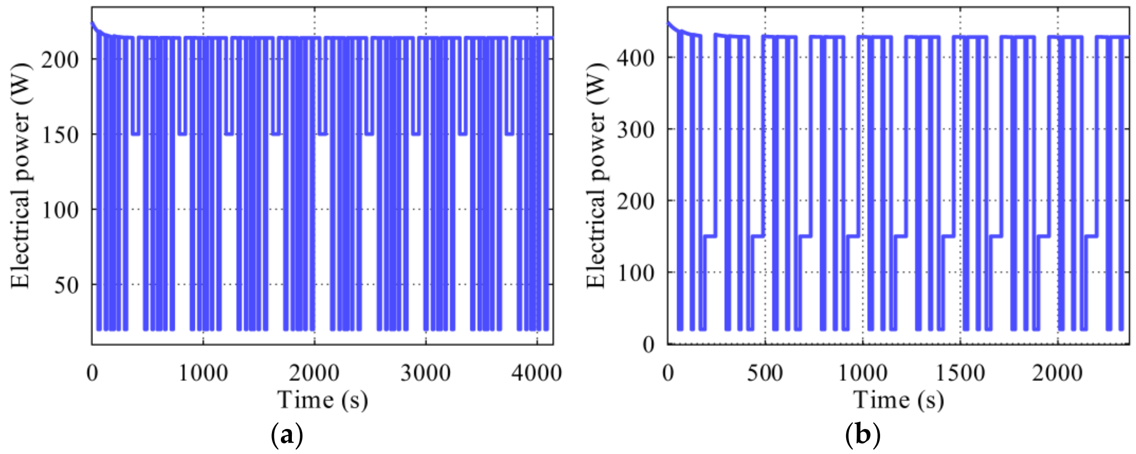

Figure 15. Electrical power consumption according for disinfection scenario 2 using two far-UVC lamps (**a**) and four far-UVC lamps (**b**).

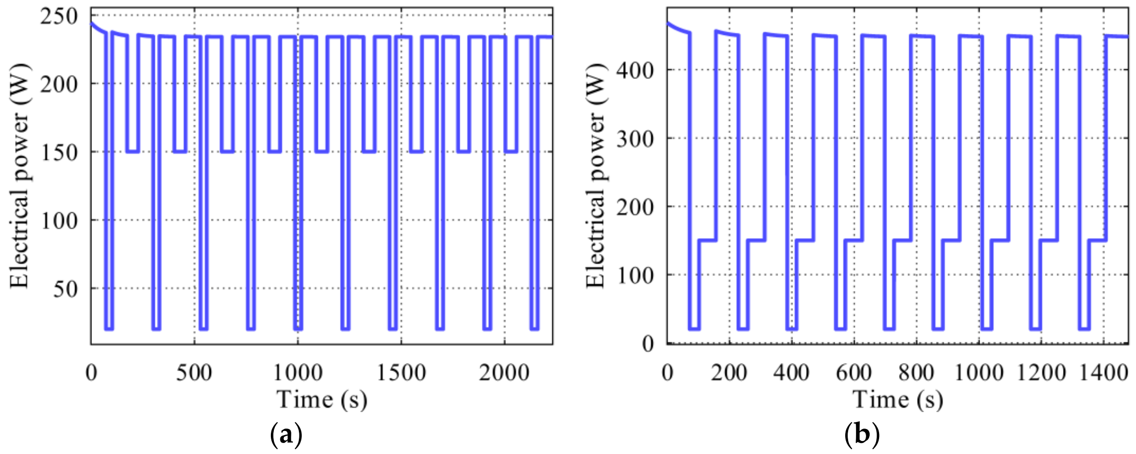

Figure 16. Electrical power consumption according for disinfection scenario 3 using two far-UVC lamps (**a**) and four far-UVC lamps (**b**).

A summary of the disinfection times and the energy consumption for each scenario is given in Table 2.

From the results obtained, we can see that disinfection scenario 2 is the least effective, with the longest disinfection time and highest energy consumption. Scenario 1 is the most efficient as it consumes the least energy and the disinfection of all bus rows is fastest with four lamps (with two lamps, disinfection takes 54 s longer than in scenario 3 due to the change in lamp position).

4. Discussion

The prototype of the disinfection system based on 222 nm wavelength far-UVC light proposed in this study offers significant contributions to the field of public transport disinfection. By addressing multiple aspects, the system provides a comprehensive approach to enhance the effectiveness and efficiency of disinfection processes while ensuring passenger safety. This paper has emphasized the importance of disinfection effectiveness by investigating the optimal far-UVC light angle and has reported a bus seat irradiation study. These efforts ensure that the disinfection system achieves the desired radiant exposure of 2 mJ/cm^2, which is crucial for effectively eliminating pathogens including the SARS-CoV-2 virus. This knowledge enables the development of disinfection protocols that maximize the system's efficiency in reducing microbial contamination on various surfaces within public buses.

From the previous studies, it is known that the long-term use of far-UVC radiation at a distinct wavelength of 222 nm for disinfection purposes can considerably impair the mechanical and visual characteristics of the surfaces intended for disinfection [27]. Energy efficiency is another key consideration in the design of a disinfection system. The proposed energy efficiency assessment model enables the simulation and optimization of electrical energy demand during the disinfection process. By accurately forecasting energy consumption, public transport authorities and operators can implement energy-saving measures and ensure the sustainable operation of a disinfection system. This will not only reduce operational costs but also contribute to environmental conservation and the overall sustainability of public transport services. Therefore, minimum disinfection durations were chosen to ensure minimum disinfection doses and energy consumption during the development of the prototype.

The analysis of different disinfection scenarios, including factors such as bus zone, disinfection time, and energy demand, provides valuable insights for practical implementation. By identifying the optimal placement of far-UVC light sources, such as in the fixed vertical position specified in the study, the disinfection system can fulfil the most efficient disinfection time and energy requirements. These findings facilitate the effective deployment of the system in real-world settings, maximizing its impact on reducing the spread of pathogens within public transport environments.

It is also important to mention that a light source with reflectors ensures that UVC radiation does not affect a person, and scenarios are analyzed when there are empty disinfected seats or the bus is empty at the end stops. When considering other scenarios that would include disinfection with people, it is necessary to evaluate the overall expected exposure limits of far-UVC in the context of legal regulations. Additionally, it should be noted that according to the manufacturer's specifications, the far-UVC lamps used in the prototype emit a minimum amount of ozone. The accumulation of ozone in an enclosed space can have adverse effects on air quality and potentially pose health risks to passengers and drivers. Therefore, additional studies are needed in the future that would allow to assess whether this ozone concentration is not excessive according to regional standards.

5. Conclusions

In this paper, a prototype of a disinfection system based on 222 nm wavelength far-UVC for public transport was proposed. The specific conclusions are as follows:

- A far-UVC based surface disinfection prototype for public buses was developed. The far-UVC light angle of the prototype was investigated, and a bus seat irradiation study was carried out in which the irradiances of individual zones were determined by evaluating both the distance between the light source and each surface to be disinfected and the disinfection time to achieve a minimum radiant exposure of 2mJ/cm^2.
- An energy efficiency assessment model of a far-UVC-based disinfection module was proposed that allows the simulation of the instantaneous electrical energy demand during the disinfection process and can be used for energy consumption optimization and forecasting.
- Three disinfection scenarios were analyzed, focusing on bus zones, disinfection times, and electrical energy demands. It was found that placing the far-UVC light source in a fixed vertical position, 75 cm from the seat and 25 cm from the center of the backrest, satisfies the optimum disinfection time and energy requirements. The disinfection of an entire bus with two lamps per row takes 38.1 min (20.6 min with four lamps) and requires 111.3 Wh of energy (109.8 Wh with four lamps).
- A subsystem that enables the real-time monitoring of occupancy levels in different areas of public buses has been developed using the Yolo v7 passenger detection algorithm. By prioritizing the disinfection process in the most crowded and frequented areas, this subsystem increases the effectiveness of the disinfection process in a bus interior.

Author Contributions: Conceptualization, D.D., M.K., A.T., Z.L., D.S., V.J., A.M., R.D. and J.G.; Data curation, D.D., M.K., A.T. and Z.L.; Formal analysis, D.D., M.K., A.T., Z.L. and J.G.; Funding acquisition, A.M. and R.D.; Investigation, D.D., M.K., A.T. and Z.L.; Methodology, D.D., M.K., A.T. and Z.L.; Project administration, A.M. and R.D.; Resources, D.D., M.K., A.T., Z.L., D.S. and V.J.; Software, D.D., M.K., A.T., Z.L. and D.S.; Supervision, D.D., M.K., A.T., Z.L. and A.M.; Validation, D.D., M.K., A.T., Z.L., D.S., V.J., A.M., R.D. and J.G.; Visualization, D.D., M.K., A.T. and Z.L.; Writing—original draft, D.D., M.K., A.T. and Z.L.; Writing review & editing, D.D., M.K., A.T., Z.L., D.S., V.J., A.M., R.D. and J.G. All authors have read and agreed to the published version of the manuscript.

Funding: This research has received funding from the European Regional Development Fund (project No 13.1.1-LMT-K-718-05-0002) under a grant agreement with the Research Council of Lithuania (LMTLT), funded as the European Union's measure in response to the COVID-19 pandemic.

Institutional Review Board Statement: Not applicable.

Informed Consent Statement: Not applicable.

Data Availability Statement: The data that support the findings of this study are available within the article.

Conflicts of Interest: The authors declare no conflict of interest.

References

1. Moreno, T.; Pintó, R.M.; Bosch, A.; Moreno, N.; Alastuey, A.; Minguillón, M.C.; Anfruns-Estrada, E.; Guix, S.; Fuentes, C.; Buonanno, G.; et al. Tracing Surface and Airborne SARS-CoV-2 RNA inside Public Buses and Subway Trains. *Environ. Int.* **2021**, *147*, 106326. [CrossRef]
2. Bertone, M.; Mikszewski, A.; Stabile, L.; Riccio, G.; Cortellessa, G.; d'Ambrosio, F.R.; Papa, V.; Morawska, L.; Buonanno, G. Assessment of SARS-CoV-2 Airborne Infection Transmission Risk in Public Buses. *Geosci. Front.* **2022**, *13*, 101398. [CrossRef]
3. Elgujja, A.A.; Altalhi, H.H.; Ezreqat, S. Review of the Efficacy of Ultraviolet C for Surface Decontamination. *J. Nat. Sci. Med.* **2020**, *3*, 8. [CrossRef]
4. Su, W.-L.; Lin, C.-P.; Huang, H.-C.; Wu, Y.-K.; Yang, M.-C.; Chiu, S.-K.; Peng, M.-Y.; Chan, M.-C.; Chao, Y.-C. Clinical Application of 222 Nm Wavelength Ultraviolet C Irradiation on SARS CoV-2 Contaminated Environments. *J. Microbiol. Immunol. Infect.* **2022**, *55*, 166–169. [CrossRef] [PubMed]
5. Matsuura, R.; Lo, C.-W.; Ogawa, T.; Nakagawa, M.; Takei, M.; Matsumoto, Y.; Wada, S.; Aida, Y. Comparison of the Inactivation Capacity of Various UV Wavelengths on SARS-CoV-2. *Biochem. Biophys. Rep.* **2022**, *32*, 101379. [CrossRef]
6. Kitagawa, H.; Nomura, T.; Nazmul, T.; Omori, K.; Shigemoto, N.; Sakaguchi, T.; Ohge, H. Effectiveness of 222-Nm Ultraviolet Light on Disinfecting SARS-CoV-2 Surface Contamination. *Am. J. Infect. Control.* **2021**, *49*, 299–301. [CrossRef]
7. Buonanno, M.; Welch, D.; Shuryak, I.; Brenner, D.J. Far-UVC Light (222 Nm) Efficiently and Safely Inactivates Airborne Human Coronaviruses. *Sci Rep* **2020**, *10*, 10285. [CrossRef]
8. Pereira, A.R.; Braga, D.F.O.; Vassal, M.; Gomes, I.B.; Simões, M. Ultraviolet C Irradiation: A Promising Approach for the Disinfection of Public Spaces? *Sci. Total Environ.* **2023**, *879*, 163007. [CrossRef]
9. Sesti-Costa, R.; Negrão, C.; von, Z.; Shimizu, J.F.; Nagai, A.; Tavares, R.S.N.; Adamoski, D.; Costa, W.; Fontoura, M.A.; da Silva, T.J.; et al. UV 254 Nm Is More Efficient than UV 222 Nm in Inactivating SARS-CoV-2 Present in Human Saliva. *Photodiagnosis Photodyn. Ther.* **2022**, *39*, 103015. [CrossRef]
10. Ramos, C.C.R.; Roque, J.L.A.; Sarmiento, D.B.; Suarez, L.E.G.; Sunio, J.T.P.; Tabungar, K.I.B.; Tengco, G.S.C.; Rio, P.C.; Hilario, A.L. Use of Ultraviolet-C in Environmental Sterilization in Hospitals: A Systematic Review on Efficacy and Safety. *Int J Health Sci (Qassim)* **2020**, *14*, 52–65.
11. Mehta, I.; Hsueh, H.-Y.; Taghipour, S.; Li, W.; Saeedi, S. UV Disinfection Robots: A Review. *Robot. Auton. Syst.* **2023**, *161*, 104332. [CrossRef] [PubMed]
12. Holland, J.; Kingston, L.; McCarthy, C.; Armstrong, E.; O'Dwyer, P.; Merz, F.; McConnell, M. Service Robots in the Healthcare Sector. *Robot.* **2021**, *10*, 47. [CrossRef]
13. Begić, A. Application of Service Robots for Disinfection in Medical Institutions. *Adv. Technol. Syst. Appl. II* **2017**, *28*, 1056–1065. [CrossRef]
14. Mahida, N.; Vaughan, N.; Boswell, T. First UK Evaluation of an Automated Ultraviolet-C Room Decontamination Device (Tru-D^{TM}). *J Hosp Infect* **2013**, *84*, 332–335. [CrossRef] [PubMed]
15. Astrid, F.; Beata, Z.; Van den Nest, M.; Julia, E.; Elisabeth, P.; Magda, D.-E. The Use of a UV-C Disinfection Robot in the Routine Cleaning Process: A Field Study in an Academic Hospital. *Antimicrob. Resist. Infect. Control.* **2021**, *10*, 84. [CrossRef]
16. Vincent, R.L.; Rudnick, S.N.; McDevitt, J.J.; Wallach, F.R. Toward a Test Protocol for Surface Decontamination Using a Mobile Whole-Room UVGI Device†. *Photochem. Photobiol.* **2021**, *97*, 552–559. [CrossRef]

17. Conte, D.; Leamy, S.; Furukawa, T. Design and Map-Based Teleoperation of a Robot for Disinfection of COVID-19 in Complex Indoor Environments. In Proceedings of the 2020 IEEE International Symposium on Safety, Security, and Rescue Robotics (SSRR), Abu Dhabi, UAE, 4–6 November 2020; pp. 276–282.
18. UVC-PURGE: A Novel Cost-Effective Disinfection Robot for Combating COVID-19 Pandemic | IEEE Journals & Magazine | IEEE Xplore. Available online: https://ieeexplore.ieee.org/document/9745041 (accessed on 6 June 2023).
19. Mohammadi, A.; Kucharski, A.; Rawashdeh, N. UVC and Far-UVC Light Disinfection Ground Robot Design for Sterilizing the Coronavirus on Vertical Surfaces. *Sensors* **2022**, 12115. [CrossRef]
20. Mehta, I.; Hsueh, H.-Y.; Kourtzanidis, N.; Brylka, M.; Saeedi, S. Far-UVC Disinfection with Robotic Mobile Manipulator. In Proceedings of the 2022 International Symposium on Medical Robotics (ISMR), Atlanta, GA, USA, 13–15 April 2022; pp. 1–8. [CrossRef]
21. Camacho, E.C.; Ospina, N.I.; Calderón, J.M. COVID-Bot: UV-C Based Autonomous Sanitizing Robotic Platform for COVID-19. *IFAC-Pap.* **2021**, *54*, 317–322. [CrossRef]
22. Ma, Y.; Xi, N.; Xue, Y.; Wang, S.; Wang, Q.; Gu, Y. Development of a UVC-Based Disinfection Robot. *Ind. Robot. Int. J. Robot. Res. Appl.* **2022**, *49*, 913–923. [CrossRef]
23. Segmenting Areas of Potential Contamination for Adaptive Robotic Disinfection in Built Environments - PMC. Available online: https://www.ncbi.nlm.nih.gov/pmc/articles/PMC7448966/ (accessed on 6 June 2023).
24. Wang, S.; Li, Y.; Ding, G.; Li, C.; Zhao, Q.; Sun, B.; Song, Q. Design of UVC Surface Disinfection Robot with Coverage Path Planning Using Map-Based Approach At-The-Edge. *Robotics* **2022**, *11*, 117. [CrossRef]
25. Recognizing Object Surface Materials to Adapt Robotic Disinfection in Infrastructure Facilities - Hu - 2022 - Computer-Aided Civil and Infrastructure Engineering - Wiley Online Library. Available online: https://onlinelibrary.wiley.com/doi/full/10.1111/mice.12811 (accessed on 6 June 2023).
26. Yates, S.F.; Isella, G.; Rahislic, E.; Barbour, S.; Tiznado, L. Effects of Ultraviolet-C Radiation Exposure on Aircraft Cabin Materials. *J. RES. NATL. INST. STAN.* **2021**, *126*, 126019. [CrossRef]
27. Drungilas, D.; Kurmis, M.; Tadzijevas, A.; Lukosius, Z.; Martinkenas, A.; Didziokas, R.; Gruode, J.; Sapalas, D.; Jankunas, V. Evaluating the Impact of 222 Nm Far-UVC Radiation on the Aesthetic and Mechanical Properties of Materials Used in Public Bus Interiors. *Appl. Sci.* **2023**, *13*, 4141. [CrossRef]
28. Wang, C.-Y.; Bochkovskiy, A.; Liao, H.-Y.M. YOLOv7: Trainable Bag-of-Freebies Sets New State-of-the-Art for Real-Time Object Detectors. *arxiv* **2022**, arXiv:2207.02696.